Collapse in High-Grade Stenosis during Pulsatile Flow Experiments*

Shunichi KOBAYASHI**, Dalin TANG*** and David N. KU****

It has been hypothesized that blood flow through high grade stenotic arteries may produce conditions in which elastic flow choking may occur. The development of atherosclerotic plaque fracture may be exacerbated by the compressive stresses during collapse. This study explored the effects of pulsatile flow on stenotic flow collapse. Pulsatile flow was produced using a gear pump controlled by a digitized physiologic waveform. Upstream and downstream mean pressures and pulsatile flow rates were measured and digitized. An improved model of arterial stenosis was created using an elastomer with an incremental modulus of elasticity matched to a bovine carotid artery in the relevant range of collapse. Additionally, the model retained a very thick wall in the stenotic region similar to arterial disease. Flow choking was observed for pulsatile pressure drops close to those previously reported for steady flow. The phase difference between flow rate and pressure between upstream and downstream of the stenosis occurred by the compliance of tube and stenosis resistance. For 80% nominal stenosis by diameter and $100+/-30$ mmHg upstream pressure, collapse occurred for average pulsatile pressure drops of 93 mmHg. Pulsatile flow experiments in this model revealed the range of conditions for the flow choking and the paradoxical collapse of the stenosis during systole with expansion during diastole. The stenosis severity was dynamic through the pulse cycle and was significantly greater under flow than the nominal severity. The results indicate that flow choking and stenotic compression may be significant in thick-walled arterial stenoses subjected to pulsatile flow.

Key Words: Atherosclerosis, Stenosis, Plaque, Pulsatile Flow, Biomechanics

1. Introduction

Atherosclerosis of the human arterial system produces localized high grade stenoses which often lead to morbid symptoms of stroke and heart attack. As the disease progresses, the plaque will encroach on the lumen and produce a stenosis. In the early stages of the disease, the arteries appear to compensate for intimal thickening by dilating the arterial wall[1]. As the plaque increases in size and encircles the lumen, the artery is no longer able to expand sufficiently to maintain a normal diameter, and the stenosis forms. Stenoses which have advanced to 75% to 90% of the lumen diameter can produce clinical symptoms of transient ischemic attacks[2),(3)] and angina pectoris[4].

As the stenosis progresses, flow is limited by losses produced by flow separation and turbulence downstream of the stenosis. In elastic arteries, the stenosis can be dynamic and increase in severity with higher flows[5]. Flow through elastic vessels is further complicated by the possibility of supercritical flow. The concept of a tube law where the elastic wall wave speed falls dramatically at transmural pressures just below zero was described by Shapiro[6]. A speed index can be defined as the ratio of the local flow velocity to the tube wave speed. The flow can induce the tube to collapse when the speed index reaches 1 and flow can transition to a supercritical state. This transition imposes a flow limitation or "choking" which is analogous to the choked flow of a compressible fluid through a Laval nozzle. Ku et al.[7] developed an inviscid model to predict the possibility of flow choking through an arterial stenosis, and Binns and Ku[8] have demonstrated the

* Received 24th May, 2004 (No. 04-4127)

** Department of Functional Machinery and Mechanics, Faculty of Textile Science and Technology, Shinshu University, 3–15–1 Tokida, Ueda, Nagano 386–8567, Japan. E-mail: shukoba@giptc.shinshu-u.ac.jp

*** Mathematical Sciences Department, Worcester Polytechnic Institute, Worcester, MA 01609, USA

**** School of Mechanical Engineering, Georgia Institute of Technology, Atlanta, GA 30332–0363, USA

collapse phenomenon in a latex tube with a rigid orifice. Thus, a compliant arterial stenosis may collapse causing a phenomenon called flow choking. Each of these hemodynamic factors will limit the flow reserve to major vital vascular beds such as the brain, the lower limbs, and heart. It is important to identify the important factors leading to this phenomenon under physiologic conditions.

The dynamic stenosis and possibility of wall compression may also lead to new stresses within the plaque itself. A likely cause of occlusive thrombosis and embolization is rupture of the collagenous plaque cap that overlies the atheroma. While the intimal cap would be typically under circumferential hoop tension for an artery with an average transmural pressure of 100 mmHg, the hemodynamic pressures in the throat of a high grade stenosis may cause the local lumenal pressure to be lower than the external tissue pressure. Thus, a negative transmural pressure would be created and the wall would be subject to damaging compression and stress concentrations[9]. Measurements of critical flow conditions would also help identify those mechanical factors that may precipitate plaque cap failure leading to strokes and heart attack.

Since the experimental models such as latex tube with rigid orifice were simple, authors have developed an experimental model that more closely approximated the arterial disease situation where the entire stenosis is compliant and the stenosis wall was not rigidly constrained[10),(11)]. We used hydrogel as the elastic thick-wall material for the new model. The model quantified conditions in which pressure drops were predominately due to separation or due to flow choking from collapse for steady flow condition.

The goals of this study were to examine flow rate, pressure and stenosis severity characteristics for the pulsatile flow condition, and clarify the influence on pulsatility of flow for elastic high grade stenosis.

2. Methods

2.1 Model

The diseased carotid artery was modeled using hydrogel shaped in the form of a stenosis. This model allowed variations in stenosis severity. The stenosis was made axisymmetric. The shape of the stenosis was approximately that of a sinusoidal curve. Considering real stenosis geometry, the thickness of stenosis should be greater than the native vessel. The hydrogel models are a more realistic stenosis model that has thick stenosis and more compliant stiffness than the model used by silicone and latex. Figure 1 illustrates the stenosis shape. Stenosis severity was expressed as the nominal percent diameter reduction of the lumen, calculated as

$$\text{Nominal stenosis severity} = (1 - Ds/D) \times 100\% \quad (1)$$

where Ds is the minimum diameter at the throat and D is the upstream diameter of 8.0 mm. The ratio of stenosis length to diameter Ls/D in the hydrogel model was 2, which is in the physiologic range. During the experiment, the stenosis model was stretched 36.5% from the initial length.

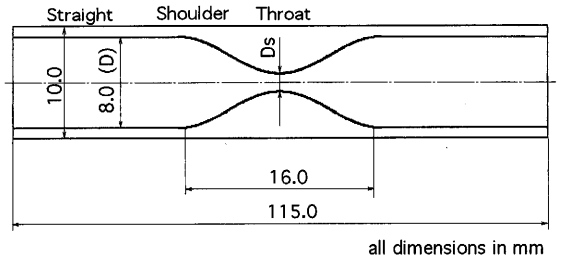

Fig. 1 Schematic representation of the stenosis model. D = 8 mm, thickness=1 mm. % Stenosis severity = $(1 - Ds/D) \times 100$ (%)

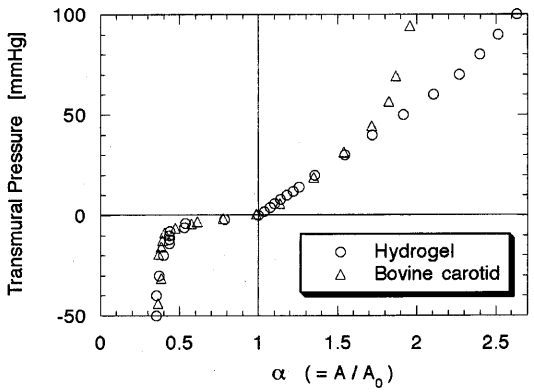

(a) Transmural pressure: from −50 to 100 mmHg

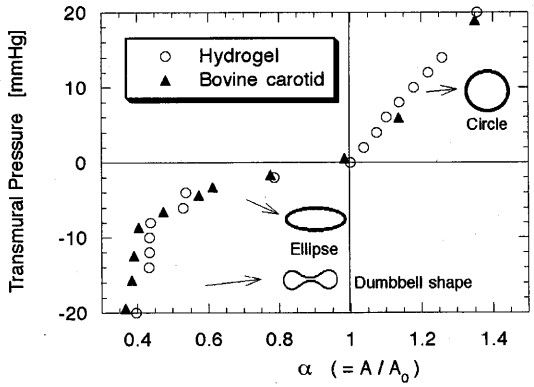

(b) Transmural pressure: from −20 to 20 mmHg (details near zero transmural pressure)

Fig. 2 Pressure – area relationship of the hydrogel tube (without stenosis) and normal bovine carotid artery. $\alpha = A/A_0$ where A is cross sectional area of the tube pressure and A_0 is cross sectional area at zero pressure. Axial stretch: 36.5% (Hydrogel tube), 34% (Normal bovine carotid artery)

Figure 2 shows the pressure-area relationship of the hydrogel tube (without stenosis) compared to a fresh normal bovine carotid artery measured by Powell[12]. The pressure-area properties of the models were determined

by digital image analysis using NIH image software. For the case of the bovine carotid was photographed from the front and top to yield two orthogonal views. The technique was fairly accurate for circular and elliptical cross-sections, but less accurate for the dumbbell shapes. While the shape changes are dependent on a whole host of factors, our goal was to gain a simple approximation of the pressure-area relationship that might be included in a mathematical description of the tube law[13]. For the case of hydrogel model, cross section area (within outer surface) was recorded by duplex ultrasound scanning (Acuson 128). Duplex ultrasound scanning is more accurate for elliptical and dumbbell cross sections. From Fig. 2 (a), the hydrogel tube is softer than normal bovine carotid over 40 mmHg of transmural pressure. However, near 0 transmural pressure (Fig. 2 (b)), the behavior of hydrogel tube is very close to bovine carotid. Thus, the hydrogel tube is very good simulation model for experiments focusing on the initial collapse of an artery. Since hydrogel has visco-elastic property, hydrogel tube has a little hysteresis behavior while increasing and decreasing of transmural pressure. In this experiment, transmural pressure was reduced progressively by decreasing internal pressure or increasing outer pressure. To eliminate for creep effect, the experiment was started several minutes later after the stretching and pressurizing.

2.2 Pulsatile flow experiments

Figure 3 shows an experimental setup. Pulsatile flow was perfused through the hydrogel stenosis model. The stenosis was mounted on rigid pipes and placed inside a water tank. The water level was 2.5 cm from the center of the stenosis model (external pressure is approx. 1.8 mmHg). Upstream constant head reservoir was pressurized as the direct current component of pulsatile flow. The computer controlled gear pump (MCP-Z, Ismatec SA Zurich) which works as alternative current component, was connected to upstream tube. The valve and the downstream constant head reservoir were set as distal resistance of the stenosis. Pressures at the upstream and downstream were measured continuously by pressure transducers (Harvard Apparatus 60-3002). The working fluid used was water at room temperature with a kinematic viscosity ν of 0.01 cm^2/s. Flow rate was measured using an ultrasound transit-time flow meter (Transonics T101) with an 8 mm in-line probe. The pressure transducers were placed on junctions the rigid tube and hydrogel, 111 mm upstream and downstream of the stenosis. The flow meter was located outside the box 163 mm upstream and downstream of the stenosis. Saggital section image of stenosis was made a video signal by Duplex ultrasound scanning (Acuson 128). For the control of gear pump, data acquisition and image grabbing of ultrasound image, we used a workstation (Gateway2000-P6, WindowsNT4.0) with A/D - D/A conversion board and video acquisition card. Control and data acquisition were operated at the same time using Labview with Imaq Software (National Instruments). As the input signal for controlling of gear pump, we digitized blood velocity in ascending aorta[14]. From the ultrasound image, lumenal diameters at upstream straight portion and throat of the stenosis, and the length of minor axis on lumenal section of end-stenosis were measured by NIH image software.

Upstream pressure and frequency, stenosis models were changed during the experiment. We defined the standard condition shown in Table 1.

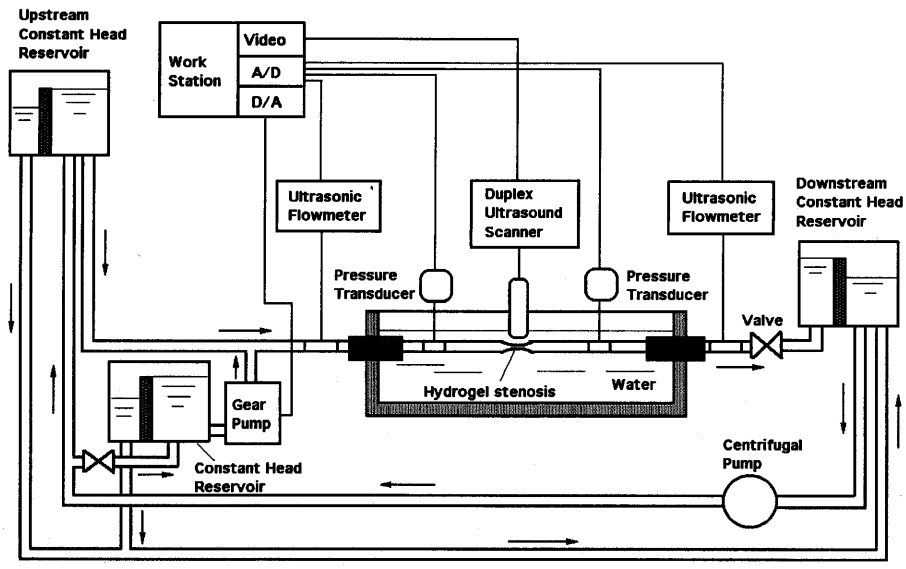

Fig. 3 Experimental setup for pulsatile flow conditions in the collapsible stenosis

Table 1 Standard condition of experiment

stenosis model	80% nominal stenosis severity
upstream pressure P_1	100 +/− 30 mmHg
frequency	1.0 Hz
frequency parameter $R(\omega/\nu)^{1/2}$ (ω: angular velocity)	12.5 – 17.6 (lumenal radius $R = 5 - 7$ mm)

3. Results

3.1 Comparison between pulsatile flow and steady flow

Figure 4 shows the downstream flow rate versus average downstream pressure in comparison with steady flow condition for 80% nominal severity stenosis. Maximum, minimum and average flow rate in pulsatile flow reach a maximum around average downstream pressure of 15 mmHg. This shows the flow choking occurs in pulsatile flow condition. For further reductions of average downstream pressure, the flow rates decrease. The average flow rate in pulsatile flow is almost the same as the flow rate in steady flow. This figure also shows that the amplitude of downstream flow rate increases with reduction of the average downstream pressure.

3.2 Straight hydrogel tube

As the basic experiment of the pulsatile flow, we measured upstream and downstream pressure for straight hydrogel tube. The results are shown in Fig. 5. The diameter of the straight tube was the same as the straight portion of the stenosis model. The tube was stretched 36.5% from 75 mm initial length. Average of downstream pressure was set to 90 mmHg. The pressure drop of 10 mmHg is caused by the area expansion and reduction at the junctions between rigid inlet and outlet tubes and the hydrogel tube. Upstream pressure and downstream pressure show qualitative agreement, and there is no significant phase difference between upstream and downstream pressures. The pressure waveform is not completely physiologic because it lacks the dicrotic notch, but it is more physiologic than a sinusoidal wave. The downstream flow wave form is similar to pressure wave form.

3.3 Pressure and flow rate

Figure 6 shows measured upstream and downstream pressure and flow rate for 80% nominal severity stenosis. The stenosis model causes a phase difference of flow rate and pressure between upstream and downstream. For the 70 mmHg average downstream pressure (Fig. 6 (a)), the phase of the maximum upstream pressure was delayed 50 degrees from the maximum upstream flow rate. The maximum of downstream pressure was delayed 70 degrees from the phase of the maximum of upstream pressure. For 0 mmHg average downstream pressure (Fig. 6 (b)), peak value of P_2 is not clear but the phase of the peak value of P_2 is the same phase as that of peak value of P_1, thus the phase difference between upstream and downstream

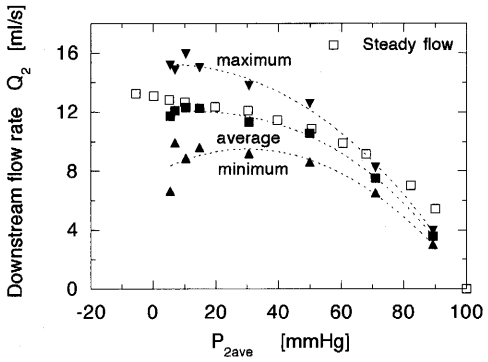

Fig. 4 Downstream flow rate versus average downstream pressure in comparison with steady flow condition for 80% nominal severity stenosis model

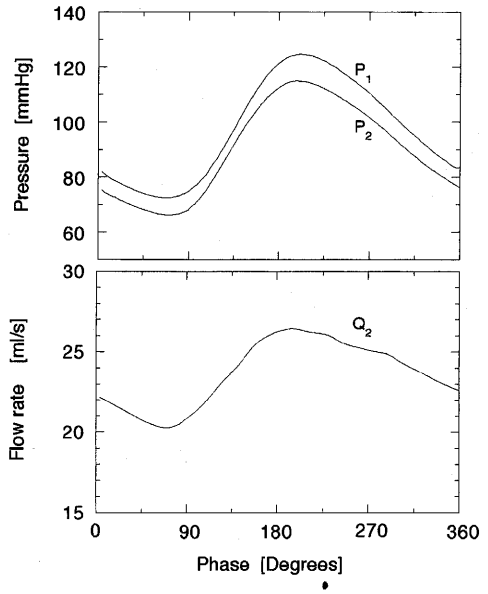

Fig. 5 Measured upstream and downstream pressure for straight hydrogel tube. Average of downstream pressure P_{2ave} = 90 mmHg. P_1: upstream pressure, P_2: downstream pressure, Q_2: downstream flow rate

maximum pressure is reduced. The phase difference in the stenosis model is accounted by the compliance of the straight portion (tube) of the stenosis model and the resistance of stenosis. The phase delay between pressure and flow rate upstream would be explained by a period to charging of fluid in upstream portion, using a *Windkessel* mode which consists of flow resistance of stenosis and compliance of hydrogel tube.

Downstream flow rate pulsatility is more attenuated for the 70 mmHg average downstream pressure, than for the 0 mmHg average downstream pressure. With the higher downstream pressure, both straight portions (upstream and downstream) absorb the change of flow rate.

3.4 Phase difference

The influence of average downstream pressure on phase differences for 80% nominal stenosis model is shown in Fig. 7. The phase difference between the max-

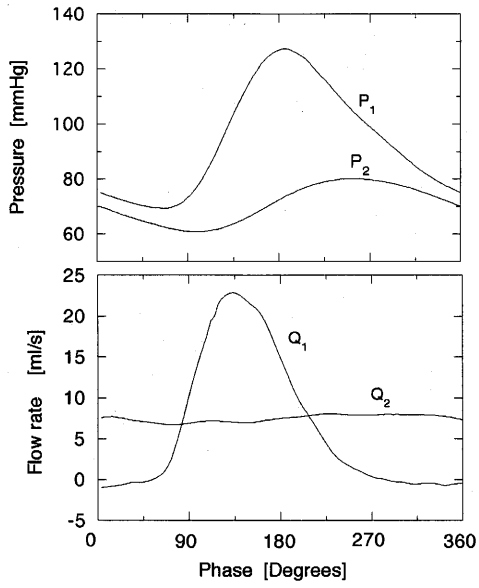

(a) $P_{2ave} = 70$ mmHg

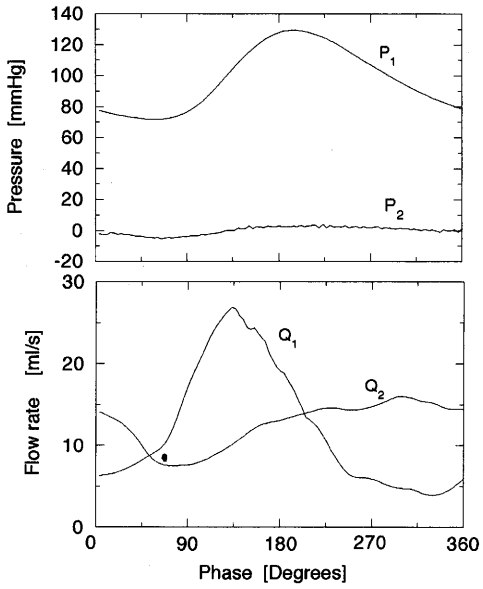

(b) $P_{2ave} = 0$ mmHg

Fig. 6 Measured upstream and downstream pressure and flow rate for 80% nominal severity stenosis. P_1: upstream pressure, P_2: downstream pressure, Q_1: upstream flow rate, Q_2: downstream flow rate

imum upstream pressure and the maximum upstream flow rate ($\varphi_{P1max} - \varphi_{Q1max}$) is constant 50 degrees for all downstream pressures. The upstream pressure was fixed 100 +/− 30 mmHg for all measurements. It appears that phase difference between upstream flow and upstream pressure is only a weak function of downstream pressure, and depends mostly on compliance of upstream portion and resistance of stenosis. The phase difference between the maximum downstream pressure and the maximum upstream pressure ($\varphi_{P2max} - \varphi_{P1max}$) is strong function of downstream pressure at low pressure, increasing from near zero degree at $P_{2ave} = 0$ to almost 70 degrees

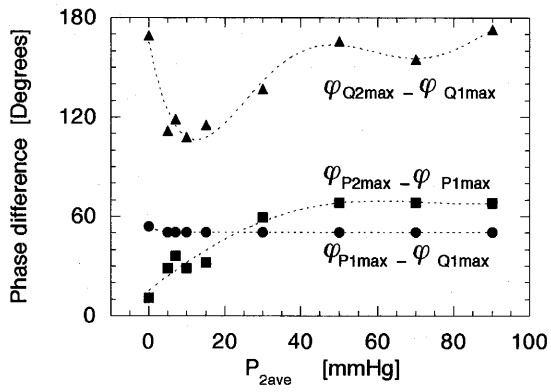

Fig. 7 Phase differences of 80% nominal stenosis model. Phase difference between maximum downstream flow rate and maximum upstream flow rate $\varphi_{Q2max} - \varphi_{Q1max}$. Phase difference between maximum upstream pressure and maximum upstream flow rate $\varphi_{P1max} - \varphi_{Q1max}$. Phase difference between maximum downstream pressure and maximum upstream pressure $\varphi_{P2max} - \varphi_{P1max}$

for $P_{2ave} > 40$ mmHg. The delay of downstream pressure reduces as the expansion by the compliance of the downstream tube reduces. The phase difference between the maximum downstream flow rate and the maximum upstream flow rate ($\varphi_{Q2max} - \varphi_{Q1max}$) is reduced by lower downstream pressure $P_{2ave} < 40$ mmHg. The decrease in downstream expansion appears to decrease phase difference, because downstream flow rate is delayed by compliance of downstream tube and resistance of the downstream valve. However, for the 0 mmHg average downstream pressure, phase difference increase immediately. It is considered that the downstream flow rate behavior is changed by the paradoxical collapse motion which is explained in the next section.

3.5 Collapse phenomenon

Two ultrasound images of cross section while collapsing are shown in Fig. 8. For the phase of 66 degrees (diastole), relatively mild ellipse cross-sectional collapse occurs downstream of the stenosis. High frequency wall motion was visible optically, but not by ultrasound. For the phase of 259 degrees (systole), the upstream side is expanded and dumbbell shape cross-sectional full collapse occurs downstream of stenosis. For 80% nominal stenosis by diameter and 100 +/− 30 mmHg upstream pressure, collapse occurred for average pulsatile pressure drops of 93 mmHg. The throat of the stenosis does not collapse easily because of its thick wall. Downstream of the stenosis, the full collapses easily due to the thin wall. Therefore, the artheriosclerosis plaque in the downstream end of stenosis would be more deformed.

In Fig. 8, we defined the length along minor axis on lumenal section of end-stenosis D_{es}. Figure 9 indicates changes in D_{es} during a period. At the normal distal pressure of $P_{2ave} = 70$ mmHg, D_{es} follows the expansion by

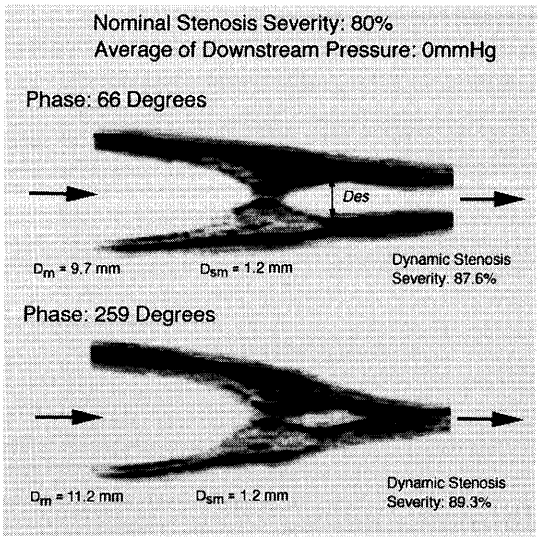

Fig. 8 Ultrasound image of Cross section while collapsing. Sagittal cross section is minor axis on lumenal section. Flow is from left to right. Upper image: ellipse cross-sectional collapse condition. Bottom image: dumbbell shape cross-sectional collapse condition. D_{es} is defined as the length of minor axis on lumenal section of end-stenosis. D_m and D_{sm} are measured diameters of upstream straight portion and throat at the same phase.

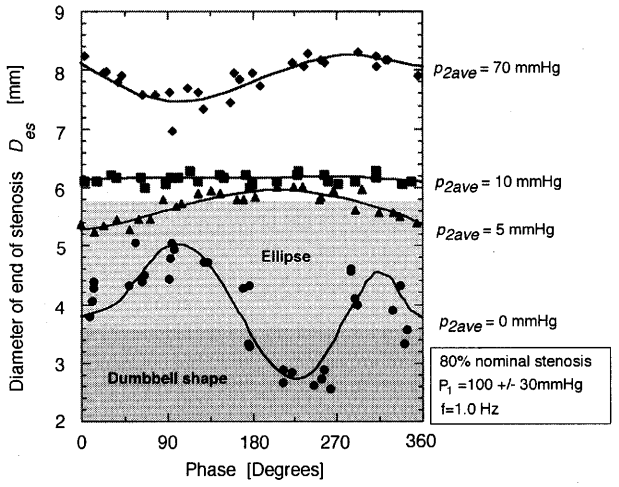

Fig. 9 Length along minor axis on lumenal section of end-stenosis D_{es} for 80% nominal stenosis severity model. D_{es} is defined in Fig. 8.

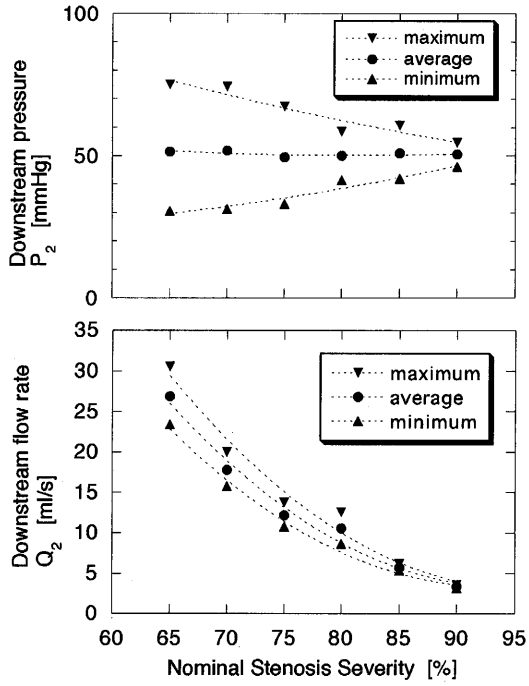

Fig. 10 Influence of stenosis severity on downstream pressure and flow rate for 50 mmHg average downstream pressure

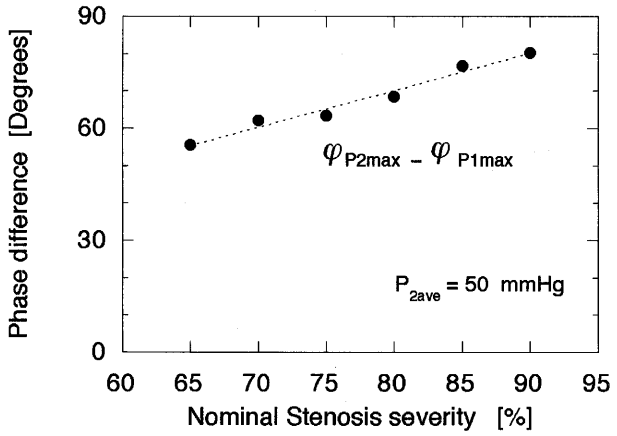

Fig. 11 Influence of stenosis severity on phase difference maximum upstream pressure and maximum downstream pressure

the downstream pressure. For lower pressure of P_{2ave} = 10 mmHg, D_{es} becomes almost constant and no collapse. At P_{2ave} = 5 mmHg, ellipse cross-sectional collapse occurs during diastole condition. For P_{2ave} = 0 mmHg (zero transmural pressure of downstream), ellipse cross-sectional collapse occurs during diastole condition, and dumbbell shape cross-sectional collapse occurs during systole condition. This phenomenon is paradoxical collapse motion of the stenosis during systole with expansion during diastole. From Fig. 6 (b), the downstream flow rate during systole is increased in spite of the large dumbbell shape cross-sectional collapse which increases distal resistance to flow.

3.6 Influence of stenosis severity and frequency

Figure 10 shows the influence of stenosis severity on downstream pressure and flow rate for 50 mmHg average downstream pressure. As the stenosis severity increases, the average flow rate is reduced. The tendency is the same as in steady flow.

Figure 11 shows the influence of stenosis severity on the phase difference between the maximum upstream pressure and the maximum downstream pressure. The phase difference increases linearly with stenosis severity. Since

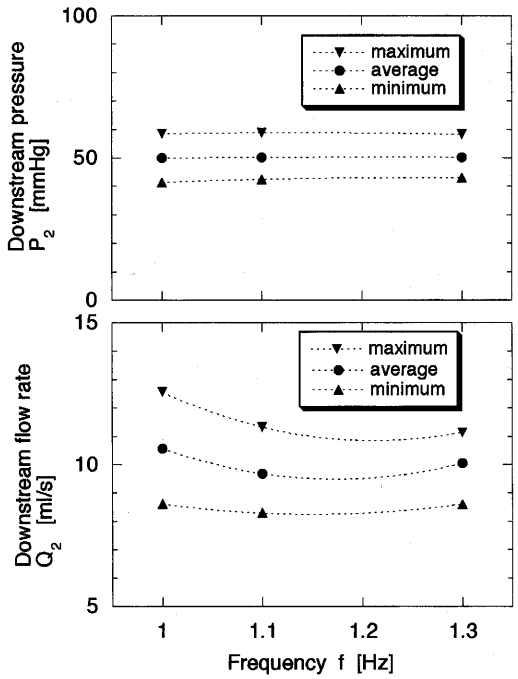

Fig. 12 Influence of frequency shifts on downstream pressure and flow rates for 50 mmHg average downstream pressure

the average downstream pressure was fixed to 50 mmHg, resistance of downstream valve increases with decrease in stenosis severity. It is considered that higher resistance downstream valve causes the delay of downstream pressure, and the decrease in stenosis severity decreases the delay of downstream pressure.

Figure 12 shows the influence of frequency shifts on downstream pressure and flow rates for 50 mmHg average downstream pressure. The downstream flow rate is not influence by variations in state range of frequency.

3.7 Dynamic stenosis severity

Figure 13 shows dynamic stenosis severity by diameter for 80% nominal stenosis severity model. The dynamic stenosis severity is defined as

$$\text{Dynamic stenosis severity} = [(D_m - D_{sm})/D_m] \times 100(\%) \quad (2)$$

where D_m and D_{sm} are measured diameters of upstream straight portion and throat at the same phase. The dynamic stenosis severity is significantly greater than nominal severity, and increases with reduction of the average downstream pressure. These tendencies are the same as in steady flow. The change in the dynamic stenosis severity during one period is similar to that in upstream pressure. The measured throat diameter changed very little compared to the upstream tube diameter, especially for high severity stenosis. Therefore, the main factor of change in dynamic stenosis severity during one period is the compliance of the straight portion.

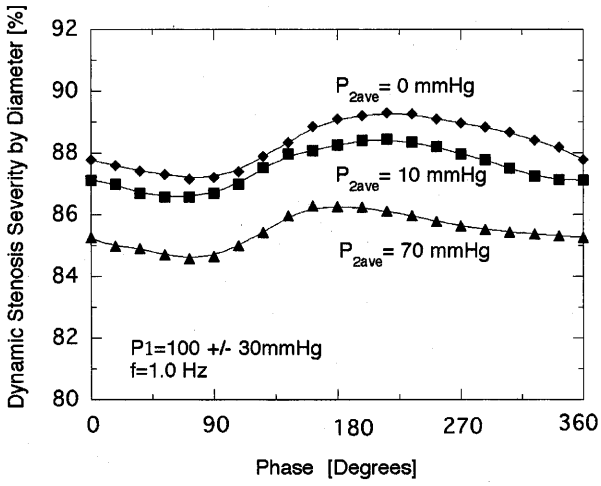

Fig. 13 Dynamic stenosis severity by diameter for 80% nominal stenosis severity model. Dynamic stenosis severity = $[(D_m - D_{sm})/D_m] \times 100$ (%). D_m and D_{sm} are measured diameters of upstream straight portion and throat at the same phase.

4. Discussion

The stenosis model shows the phase difference, this phenomenon is caused by compliance of hydrogel tube and stenosis resistance. This stenosis model would be modeled by *Windkessel* models of upstream and downstream, and are consists of compliance of upstream portion and resistance of stenosis, compliance of downstream portion and distal resistance, respectively. Phase difference between upstream pressure and flow rate depends on compliance of upstream straight portion and stenosis resistance. Phase difference between downstream pressure and flow rate depends on compliance of downstream straight portion and the downstream valve. However, for 0 mmHg average downstream pressure as the condition of paradoxical collapse motion, the phase of downstream flow rate has changed: During the systole, the downstream flow rate is on increasing in spite of the large dumbbell shape cross-sectional collapse which increases distal resistance to flow. After the dumbbell shape cross-sectional collapse, the resistance reduces and the downstream flow rate increases and peaks at 310 degrees.

Since the hydrogel tube is softer than carotid artery in positive transmural pressure (Fig. 2) and the diameter of hydrogel is greater than artery, the capacitance of the stenosis model is greater than artery. Bisides, the flow rate was greater by the greater diameter and low viscosity using water. For the future study, Reynolds number and frequency parameter of the experiment should be closer to those of the human carotid artery. For the greater capacity of the stenosis model, the phase difference of the stenosis model should be greater than artery. However, small phase difference of flow and pressure, attenuation of downstream pressure by the stenosis *in vivo* are predicted from this re-

sult. The length of the compliant tube is also significant parameter for the capacitance of artery. The length of the straight tube of this experiment is about 70 mm, shorter straight portion of the stenosis leads low capacitance. For the stenosis near the bifurcation, the phase difference is smaller because of shorter upstream length from the stenosis. On the contrary, for the stenosis which has longer upstream artery is likely to change difference and attenuated. Siebes et al.[15] were measured upstream and downstream flow rate and pressure of eccentric rigid stenoses plugged in silicone tube for pulsatile flow condition. The phase difference was not appeared because of high stiffness (approx. 2.3 times greater than artery) and low frequency (0.24 Hz). High stiffness causes low capacitance, low frequency leads low $\Delta P_1(t)/\Delta t$.

From the result of downstream flow rate, the average flow rate is close to steady flow condition. Our study for the steady flow showed stenosis severity is the most dominant factor for flow choking[10),(11]. The flow rate was reduced larger by high severity of stenosis for the pulsatile flow condition. Previous theoretical and experimental studies showed that the collapse phenomenon does not depend strongly on upstream pulsatility[12),(16]. The average downstream pressure to collapse was almost same as downstream pressure for steady flow condition. Therefore, simple steady flow model is sufficient to examine flow choking and collapse condition.

However, discussion of the phase to collapse is also important. Binns and Ku[8] made experimental observations of tube collapse induced by rigid stenosis. Their experiments used a pressure pulse 80 +/− 20 mmHg. Paradoxical collapse motion just distal to the stenosis occurred during the high flow systolic phase of the pulsatile cycle. This motion is also appeared in theoretical study by Downing and Ku[16]. For the phase and degree of collapse of this pulsatile flow experiment, there were two behaviors: (a) For 5 mmHg average downstream pressure, ellipse cross-sectional collapse occurs in diastole. (b) For 0 mmHg average downstream pressure (around zero transmural pressure), ellipse cross-sectional collapse occurs during diastole condition, and dumbbell shape cross-sectional collapse occurs during systole condition as the paradoxical collapse motions. Collapse is likely occurs in lower transmural pressure of distal side of stenosis. In this experiment, average downstream pressure of collapse was less than 7 mmHg. As for the distal pressure, the stump pressure of carotid artery was reported that 0 to 25 mmHg from 18% of patients[17]. Thus, the low downstream pressures in these experiments were in physiological range. Tissue pressure was reported between −7 and 13 mmHg[18]. High external condition may occur with coughing or a Valsalsa's maneuver that raise the external pressure around a carotid or coronary artery to over 50 mmHg[8].

Collapse was located near the downstream end of stenosis and in the straight tube further downstream of stenosis. This location is the same as in steady flow. The plaque may be subject to cyclic compression even if the location of collapse is end of the stenosis. Since concentric stenosis is more stable than eccentric stenosis, it is likely considered that the location of collapse for eccentric stenosis will be closer to the throat than in a concentric stenosis, and the paradoxical collapse motion is also likely to occur.

We have not changed the total length of the stenosis model. The influence of the total stenosis model is needed for the detailed experiment. To evaluate the influence of elasticity of the stenosis model, the rigid stenosis model with the same dimension is required. Since the phase difference is not independent of the frequency parameter respect to the pressure gradient, the comparison with the rigid stenosis model with change in the frequency parameter is required in the future.

In conclusion, we have shown that the flow choking and collapse phenomenon in thick-walled arterial stenosis model on pulsatile flow condition. The phase difference of flow rate and pressure between upstream and downstream, dynamic stenosis severity and the phase to collapse and its degree were clarified. It is suggested that plaque compression and rupture by cyclic collapse are likely undergo at downstream end of stenosis. This mechanical environment should be included in studies of end-stage arterial disease.

References

(1) Glagov, S., Zarins, C.K., Giddens, D.P. and Ku, D.N., Hemodynamics and Atherosclerosis Insights and Perspectives Gained from Studies of Human Arteries, Arch. Path. Lab. Med., Vol.112 (1988), pp.1018–1031.

(2) North American Symptomatic Carotid Endarterectomy Trial Collaborators, Beneficial Effect of Carotid Endarterectomy Patients with High-Grade Carotid Stenosis, New England J. Med., Vol.325 (1991), pp.445–463.

(3) MRC European Carotid Surgery Trial, Interim Results for Symptomatic Patients with Severe (70–99%) or Mid (0–29%) Stenosis, Lancet, Vol.337 (1991), pp.1235–1243.

(4) Rutherford, J.D. and Braunwald, E., Chronic Ischemic Heart Disease, Heart Disease, Fourth Edition, Edited by Braunwald, E.W.B., (1992), Saunders Co., Philadelphia.

(5) Gould, K.L., Collapsing Coronary Stenosis a Starling Resistor, International Journal of Cardiology, Vol.2 (1982), pp.39–42.

(6) Shapiro, A.H., Steady Flow in Collapsible Tubes, ASME Journal of Biomechanical Engineering, Vol.99 (1977), pp.126–147.

(7) Ku, D.N., Zeigler, M.N. and Downing, J.M., One-Dimensional Steady Inviscid Flow through a Stenotic Collapsible Tube, ASME Journal of Biomechanical Engineering, Vol.112 (1990), pp.444–450.

(8) Binns, R.L. and Ku, D.N., The Effect of Stenosis on Wall Motion: A Possible Mechanism of Stroke and Transcient Ischemic Attack, Arteriosclerosis, Vol.9 (1989), pp.842–847.

(9) Aoki, T. and Ku, D.N., Collapse of Diseased Arteries with Eccentric Cross Section, Journal of Biomechanics, Vol.26, No.2 (1993), pp.133–142.

(10) Kobayashi, S., Kulbaski, M.J., Tang, D. and Ku, D.N., Hemodynamics and Wall Compression in High Grade Arterial Stenosis, International Journal of Cardiovascular Medicine and Science, Vol.1, No.1 (1997), p.32.

(11) Ku, D.N., Kobayashi, S. and Mijovic, B., Compression from Pressure Conditions in Models of Arterial Disease, Annals of Biomedical Engineering, Vol.25, No.1 (1997), p.127.

(12) Powell, B.E., Experimental Measurements of Flow through Stenotic Collapsible Tubes, Master's Thesis, School of Mechanical Engineering, GeorgSchool of Mechanical Engineering, Georgia Institute of Technology, (1991).

(13) Elad, D. and Kamm, R.D., Parametric Evaluation of Forced Expiration Using a Numerical Model, ASME Journal of Biomechanical Engineering, Vol.111, August (1989), pp.192–199.

(14) Mills, C.J., Gabe, I.T., Gault, J.H., Mason, D.T., Ross, J., Jr., Braunwald, E. and Shillingford, J.P., Pressure-Flow Relationships and Vascular Impedance in Man, Cardiovascular Res., Vol.4 (1970), pp.405–417.

(15) Siebes, M., Campbell, C.S. and D'Argenio, D.Z., Fluid Dynamics of a Partially Collapsible Stenosis in a Flow Model of the Coronary Circulation, ASME Journal of Biomechanical Engineering, Vol.118, Nov. (1996), pp.489–497.

(16) Downing, J.M. and Ku, D.N., Effects of Frictional Losses and Pulsatile Flow on the Collapse of Stenotic Arte Pulsatile Flow on the Collapse of Stenotic Arteries, ASME Journal of Biomechanical Engineering, Vol.119, August (1997), pp.317–324.

(17) Hafner, C.D., Minimizing the Risks of Carotid Endarterectomy, Journal of Vascular Surgery, Vol.1 (1984), pp.392–397.

(18) Guyton, A.C., Textbook of Medical Physiology, (1986), pp.354–356, WB Saunders, Philadelphia.